Long Alkyl Side-Chains Impede Exciton Interaction in Organic Light Harvesting Crystals

*Kalaivanan Nagarajan,‡ Gopika Gopan,‡ Rijo T. Cheriya, and Mahesh Hariharan**

School of Chemistry, Indian Institute of Science Education and Research Thiruvananthapuram, CET Campus, Sreekaryam, Thiruvananthapuram, Kerala, INDIA 695016. E-mail: mahesh@iisertvm.ac.in

Electronic Supplementary Information

Materials and methods

All chemicals were obtained from commercial suppliers and used as received without further purification. All reactions were carried out in oven-dried glassware prior to use and wherever necessary, were performed under dry nitrogen in dried, anhydrous solvents using standard gastight syringes, cannulae, and septa. Solvents were dried and distilled by standard procedures. TLC analysis were performed on precoated aluminium plates of silica gel 60 F254 plates (0.25 mm, Merck) and developed TLC plates were visualized under short and long wavelength UV lamps. Flash column chromatography was performed using silica gel of 200-400 mesh employing a solvent polarity correlated with the TLC mobility observed for the substance of interest. Yields refer to chromatographically and spectroscopically homogenous substances. Melting points were obtained using a capillary melting point apparatus and are uncorrected. IR spectra were recorded on a Shimadzu IRPrestige-21 FT-IR spectrometer as KBr pellets. ^{1}H and ^{13}C NMR spectra were measured on a 500 MHz Bruker advanced DPX spectrometer. Internal standard used for ^{1}H and ^{13}C NMR is 1,1,1,1-tetramethyl silane (TMS). All the elemental analyses were performed on Elementar Vario MICRO Cube analyzer. All values recorded in elemental analyses are given in percentages. Reference standard used for elemental analysis is 4-aminobenzenesulphonic acid (sulphanilic acid).

Spectral Measurements: Absorption spectra were recorded on Shimadzu UV-3600 UV-VIS-NIR while fluorescence and excitation spectra were performed on Horiba Jobin Yvon Fluorolog spectrometers respectively. Fluorescence lifetime measurements were carried out in an IBH picosecond single photon counting system. The fluorescence decay profiles were de-convoluted using IBH data station software version 2.1, and fitted with exponential decay, minimizing the $\chi 2$ values of the fit to 1 ± 0.05. All spectroscopic experiments were performed by using standard quartz cuvettes of path length 1cm for solution in dried and distilled solvents. The solution state fluorescence quantum yields were determined by using optically matched solutions. Nile red in 1,4-dioxane (Φ_f = 0.7)[1] is used as the standard for quantum yield measurement of **NP** derivatives in solution state. The solid state quantum yield of crystalline **NP** derivatives was measured using an integrating sphere for which the accuracy was verified using tris(8-hydroxyquinolinate)aluminium (Alq_3) as a standard and is determined to be 0.37 ± 0.04 (reported quantum yield Φ_f = 0.40).[2] Radiative (k_r) and non-radiative (k_{nr}) decay rate constants can be calculated by using the equations 3 and 4.

$$\Phi = \frac{k_r}{k_r + k_{nr}} \quad (1)$$

$$\tau_f = \frac{1}{k_r + k_{nr}} \quad (2)$$

$$k_r = \frac{\Phi}{\tau_f} \quad (3)$$

$$k_{nr} = \frac{1}{\tau_f} - k_r \quad (4)$$

where Φ is the fluorescence quantum yield and τ_f is the fluorescence lifetime. In case of multi exponential decay as in the case of crystalline **NP** derivatives, the weighted average of the fluorescence lifetime values was used for estimation of rates of radiative and non-radiative processes which could be calculated using equation 5,[3]

$$\tau_f = \frac{\alpha_1\tau_1^2 + \alpha_2\tau_2^2 + \alpha_3\tau_3^2 + \ldots}{\alpha_1\tau_1 + \alpha_2\tau_2 + \alpha_3\tau_3 + \ldots} \quad (5)$$

where α= amplitude corresponding to the fluorescence lifetime (τ_f) decay.

Fluorescence anisotropy measures the depolarisation of the fluorescence emission. The main reasons for depolarisation include the energy transfer to another molecule with a different orientation or molecular rotation caused by Brownian motion. Molecular motion depends on local environmental factors, such as viscosity and molecular confinement, and the size of the molecule. Thus a measurement of fluorescence anisotropy is useful in obtaining information concerning molecular size, mobility and energy migration in crystals. In the simplest case the change of anisotropy with time is given by,

$$r(t) = r_0 exp(-t/\tau_r) \quad (6)$$

where r_0 is the initial anisotropy and ranges from 0.4 (parallel transition dipoles) to -0.2 (perpendicular dipoles). Note that, these values are different if using 2-photon excitation. τ_r is the rotational correlation time, which can be considered a measure of anisotropy memory. The excitation laser used for crystalline **NP** derivatives was 375 nm laser with a pulse duration <100 ps. Any decay that occurs within the pulse width of the excitation source cannot be measured.

Analysis of Chromaticity Index: Coordinates (x, y, z) for chromaticity are acquired by calculating the fractional component of the tristimulus values: x = X/(X+Y+Z), y = Y/(X+Y+Z), z = Z/(X+Y+Z). X, Y, Z are the CIE 1931 tristimulus values. By convention, chromicity coordinates (x, y) denote the two dimensional plot CIE 1931 colour space chromaticity diagram.

X-ray Crystallography: High-quality specimens of appropriate dimensions were selected for the X-ray diffraction experiments. Crystallographic data collected are presented in the supplementary information. Single crystals were mounted using oil (Infineum V8512) on a glass fibre. All measurements were made on a CCD area detector with graphite monochromated Mo Kα radiation. The data was collected using Bruker APEXII detector and processed using APEX2 from Bruker. All structures were solved by direct methods and expanded using Fourier techniques. The non-hydrogen atoms were refined anisotropically. Hydrogen atoms were included in idealized positions, but not refined. Their positions were constrained relative to their parent atom using the appropriate HFIX command in SHELXL-97.The full validation of CIFs and structure factors of **NP** derivatives were performed using the CheckCIF utility and found to be free of major alert level. 3D structure visualization and the exploration of the crystal packing of **NP** derivatives were carried out using Mercury 3.8.

Hirshfeld Analysis: Important intermolecular interactions within the crystal structure of **NP** derivatives were identified through Hirshfeld surface analysis using Crystal Explorer 3.1. The Hirshfeld surface is defined as a set of points in 3D space where the ratio of promolecule and procrystal electron densities is equal to 0.5. The exploration of intermolecular contacts is provided by mapping normalized contact distances (d_{norm}), which is a function of a closest distance from the point to the nucleiinterior (d_i) and exterior (d_e) to the surface as well as on the van der Waals radii (r^{vdw}). 2D fingerprint which were generated by deriving from the Hirshfeld surface by plotting the fraction of points on the surface as the function of d_i and d_e which provide a visual summary of intermolecular contacts within the crystal.

Materials Science Suite: Materials Science Suite: Materials Science Suite 2016-2 provides diverse set of tools for predicting and computing reactivity and properties of chemical systems. It encompasses tools to facilitate in generating all the steps in a chemical simulation, including structure generation, property prediction followed by data analyses. The core simulation engine, Jaguar[4] is a high performance ab intio quantum mechanical package commercially produced and maintained by Schrodinger Inc. Employing psuedospectral approach, Jaguar estimates the Coulomb and exchange terms, providing significant advantages of exact exchange terms. Calculation of electronic coupling constants were performed at B3LYP-D3/6-311G**+ level of theory using the crystal structure data.[5]

DFT calculations of charge transfer electronic coupling constants were done using the optoelectronics panel of Jaguar package in Materials Science Suite 2016-2. Electronic coupling between different monomers in the crystal structure of NP derivatives were calculated at B3LYP-D3/6-311G+(d,p) level of theory using the mol2 files from crystal structure as the input. Herein, we have calculated the charge

transfer electronic coupling in distinguishable dimers of NP derivatives by using the standard computational techniques available in the Schrodinger Suite.

Synthesis, procedure and characterization:

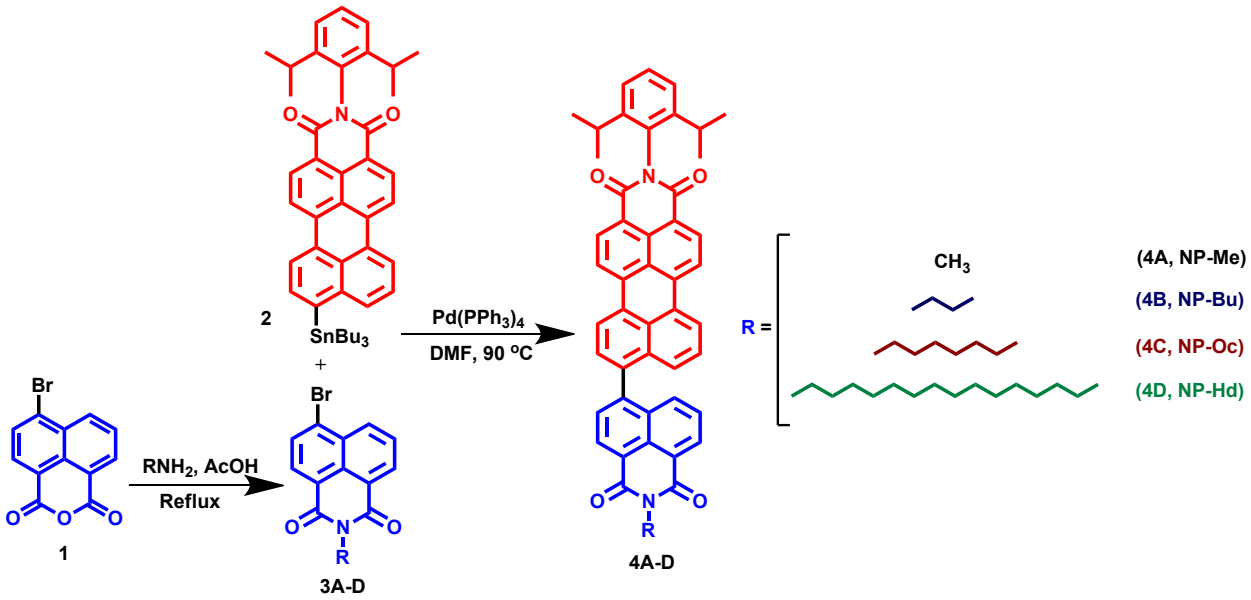

Scheme S1. Shows the synthesis of **NP-Me**, **NP-Bu**, **NP-Oc** and **NP-Hd**.

Synthetic details of N-(2,6-diisopropylphenyl)-9-(tributylstannyl)perylene-3,4-dicarboximide (**1**) was described in previously reported procedure.[6]

Preparation of 4-Bromo-N-methyl-naphthalene-1,8-dicarboximide (3A) : To a solution of 4-bromo-1,8-naphthalic anhydride **(1)** (1.00 g, 3.60 mmol) in 100 mL water, methyl amine (0.56 g, 18.00 mmol) was added. This reaction mixture was heated at 60 °C for 12 h following which it was filtered and the precipitate was washed with water and dried. The crude product was then purified by column chromatography (silica gel, EtOAc:petroleum ether 1:1) to afford compound **3A** (0.93 g, 90%) as a white solid. m. p. 183 °C; ^{1}H NMR (500 MHz, $CDCl_3$) δ: 8.69 (d, J = 7.00 Hz, 1H), 8.59 (d, J = 8.50 Hz, 1H), 8.44 (t, J = 7.00 Hz, 1H), 8.06 (d, J = 7.50 Hz, 1H), 7.87 (t, J =7.50 Hz, 1H), 3.58 (s, 3H); ^{13}C NMR (125 MHz, $CDCl_3$) δ: 163.87, 163.85, 133.31, 132.02, 131.20, 131.10, 130.62, 130.30, 128.86, 128.07, 122.98, 122.11, 27.10; IR (KBr): 3059, 2947, 1699, 1664, 1589,1568, 1400, 1361, 1286, 1226, 1031, 777 cm^{-1}; Anal. Calcd. for $C_{13}H_8BrNO_2$: C, 53.82; H, 2.78; N, 4.83%. Found: C, 53.55; H, 2.36; N, 4.60%.

Preparation of 4-Bromo-N-butyl-naphthalene-1,8-dicarboximide (3B): To a solution of 4-bromo-1,8-naphthalic anhydride (**1**) (1.00 g, 3.60 mmol) in 30 mL acetic acid, butan-1-amine (1.31 g, 18.00 mmol) was added. This reaction mixture was heated at 119 °C for 12 h followed by cooling to room temperature. It was then poured in to water, filtered and the precipitate was washed with water and dried. The crude product was then purified by column chromatography (silica gel, EtOAc:petroleum ether 1 : 1) to afford compound **3B** (0.71 g, 60%) as a white solid. m. p. 98 °C; ^{1}H NMR (500 MHz, $CDCl_3$) δ: 8.56 (d, J = 7.50 Hz, 1H), 8.46 (d, J = 8.50 Hz, 1H), 8.31 (d, J = 8.00 Hz, 1H), 7.94 (d, J = 8.00 Hz, 1H), 7.75 (t, J = 8.00 Hz, 1H), 4.09 (t, J = 7.50 Hz, 2H), 1.67 – 1.61 (m, 2H), 1.39 – 1.35 (m, 2H), 0.90 (t, J = 7.50 Hz, 3H); ^{13}C NMR (125 MHz, $CDCl_3$) δ: 162.57, 162.54, 132.13, 130.94, 130.14, 130.04, 129.56, 129.12, 127.94, 127.02, 122.12, 121.26, 39.35, 29.14, 19.34, 12.81; IR (KBr): 2953, 2868, 1696, 1662, 1589, 1570, 1504, 1460, 1346, 1265, 1228, 1074, 941, 854, 781, 746 cm^{-1}; Anal. Calcd. for $C_{16}H_{14}BrNO_2$: C, 57.85; H, 4.25; N, 4.22%. Found: C, 57.51; H, 3.96; N, 3.98%.

Preparation of 4-Bromo-N-octyl-naphthalene-1,8-dicarboximide (3C): To a solution of 4-bromo-1,8-naphthalic anhydride (**1**) (1.00 g, 3.60 mmol) in 30 mL acetic acid octan-1-amine (2.32 g, 18.00 mmol) was added. This reaction mixture was heated at 119 °C for 12 h followed by cooling to room temperature. It was then poured in to water, filtered and the precipitate was washed with water and dried. The crude product was then purified by column chromatography (silica gel, EtOAc:petroleum ether 1 : 1) to afford compound **3C** (0.84 g, 60%) as a white solid. m. p. 82 °C; ^{1}H NMR (500 MHz, $CDCl_3$) δ: 8.56 (d, J = 8.00 Hz, 1H), 8.48 (d, J = 8.50 Hz, 1H), 8.33 (d, J = 8.00 Hz, 1H), 7.96 (d, J = 7.50 Hz, 1H), 7.77 (t, J = 8.00 Hz, 1H), 4.08 (t, J = 7.50 Hz, 2H), 1.66 – 1.63 (m, 2H), 1.36 – 1.33 (m, 2H), 1.23 – 1.18 (m, 8H), 0.79 (t, J = 7.50 Hz, 3H); ^{13}C NMR (125 MHz, $CDCl_3$) δ: 163.60, 163.58, 133.18, 131.99, 131.18, 131.08, 130.63, 129.02, 128.06, 123.02, 122.34, 40.65, 31.82, 29.33, 29.21, 28.10, 27.14, 22.64, 14.08; IR (KBr): 2920, 2850, 1701, 1649, 1591, 1458, 1355, 1228, 1049, 785 cm^{-1}; Anal. Calcd. for $C_{20}H_{22}BrNO_2$: C, 61.86; H, 5.71; N, 3.61%. Found: C, 61.51; H, 5.46; N, 3.38%.

Preparation of 4-Bromo-N-hexadecyl-naphthalene-1,8-dicarboximide (3D): To a solution of 4-bromo-1,8-naphthalic anhydride (**1**) (1.00 g, 3.60 mmol) in 100 mL acetic acid hexadecan-1-amine (4.34 g, 18.00 mmol) was added. This reaction mixture was heated at 119 °C for 12 h followed by cooling to room temperature. It was then poured in to water, filtered and the precipitate was washed with water and dried. The crude product was then purified by column chromatography (silica gel, EtOAc:petroleum ether 4 : 1) to afford compound **3D** (1.08 g, 60%) as a white solid. m. p. 74 °C; ^{1}H NMR (500 MHz, $CDCl_3$) δ: 8.68 (d, J = 7.00 Hz, 1H), 8.57 (d, J = 8.50 Hz, 1H), 8.44 (d, J = 7.50 Hz, 1H), 8.06 (d, J = 8.00 Hz, 1H), 7.87 (t, J = 7.00 Hz, 1H), 4.19 (t, J = 8.00 Hz, 2H), 1.78 – 1.72 (m, 2H), 1.47 – 1.45 (m, 2H), 1.43 – 1.41 (m, 2H), 1.31 – 1.27 (m, 22H,) 0.91 (t, J = 7.00 Hz, 3H); ^{13}C NMR (125 MHz, $CDCl_3$) δ: 163.62, 163.60,

133.19, 132.00, 131.20, 131.09, 130.65, 130.16, 129.03, 128.07, 123.21, 122.35, 40.65, 31.92, 29.64, 29.63, 29.61, 29.55, 29.37, 29.35, 28.10, 27.14, 22.69, 14,12; IR (KBr): 2920, 2850, 1703, 1660, 1591, 1465, 1352, 1352, 1230, 1082, 777 cm^{-1}; Anal. Calcd. for $C_{28}H_{38}BrNO_2$: C, 67.19; H, 7.65; N, 2.80%. Found: C, 67.45; H, 7.45; N, 2.51%.

Preparation of 9-(4-(N-methyl)-naphthalene-1,8-dicarboximide)yl)-N-(2,6-diisopropylphenyl)-perylene-3,4-dicarboximide (4A): A solution of N-(2,6-diisopropylphenyl)-9-(tributylstannyl))perylene-3,4-dicarboximide **(2)** (0.686 g, 0.89 mmol), 4-Bromo-N-methyl-naphthalene-1,8-dicarboximide **(3A)** (0.32 g, 1.12 mmol) and $Pd(PPh_3)_4$ (10.28 mg, 0.0089 mmol) in 50 mL DMF was heated at 90 °C for 2 days. The solvent was removed under reduced pressure and the residue was purified by column chromatography (silica gel, EtOAc:petroleum ether 1:1) to afford compound **4A** (0.46 g, 70%) as a yellow-orange solid. m. p. > 300 °C; ^{1}H NMR (500 MHz, $CDCl_3$) δ: 8.72 (d, J = 7.50 Hz, 1H), 8.66 – 8.56 (m, 4H), 8.51 (d, J = 7.50 Hz, 1H), 8.46 (d, J = 7.50 Hz, 2H), 7.87 – 7.77 (m, 2H), 7.62 (d, J = 7.50 Hz, 1H), 7.57 (t, J = 7.50 Hz, 1H), 7.45 – 7.40 (m, 2H), 7.34 (d, J = 8.50 Hz, 1H), 7.28 (d, J = 7.5 Hz, 2H), 3.57 (s, 3H), 2.73 – 2.69 (m, 2H), 1.13 – 1.11 (m, 12H); ^{13}C NMR (125 MHz, $CDCl_3$) δ: 164.41, 163.25, 162.91, 144.70, 144.67, 143.30, 138.13, 136.27, 135.99, 132.40, 131.55, 131.15, 131.12, 130.50, 130.11, 129.91, 129.73, 129.51, 129.00, 128.69, 128.49, 128.14, 127.92, 127.89, 127.38, 127.25, 126.64, 126.28, 125.97, 123.09, 123.03, 122.12, 121.95, 121.68, 120.49, 120.36, 119.74, 119.62, 28.14, 26.14, 23.02, 23.00; IR (KBr): 3064, 2960, 1701, 1662, 1598, 1357, 1035, 812, 756 cm^{-1}; Anal. Calcd. for $C_{47}H_{34}N_2O_4$: C, 81.72; H, 4.96; N, 4.06%. Found: C, 81.25; H, 5.27; N, 3.86%.

Preparation of 9-(4-(N-butyl)-naphthalene-1,8-dicarboximide)yl)-N-(2,6-diisopropylphenyl)-perylene-3,4-dicarboximide (4B): A solution of N-(2,6-diisopropylphenyl)-9-(tributylstannyl))perylene-3,4-dicarboximide **(2)** (0.686 g, 0.89 mmol), 4-Bromo-N-butyl-naphthalene-1,8-dicarboximide **(3B)** (0.37 g, 1.11 mmol) and $Pd(PPh_3)_4$ (10.28 mg, 0.0089 mmol) in 50 mL DMF was heated at 90 °C for 2 days. The solvent was removed under reduced pressure and the residue was purified by column chromatography (silica gel, EtOAc:petroleum ether 1:2) to afford compound **4B** (0.32 g, 50%) as a red-orange solid. m. p. > 300 °C; ^{1}H NMR (500 MHz, $CDCl_3$) δ: 8.69 (d, J = 7.50 Hz, 1H), 8.67 – 8.64 (m, 2H), 8.60 – 8.56 (m, 2H), 8.51 (d, J = 8.00 Hz, 1H), 8.47 (d, J = 8.00 Hz, 2H), 7.82 – 7.77 (m, 2H), 7.61 (d, J = 7.50 Hz, 1H), 7.57 (t, J = 8.00 Hz, 1H), 7.46 – 7.43 (m, 2H), 7.35 (d, J = 8.50 Hz, 1H), 7.28 (d, J = 8.00 Hz, 2H), 4.19 (t, J = 8.00 Hz, 2H), 2.72 – 2.70 (m, 2H), 1.74 – 1.68 (m, 2H), 1.46 – 1.41 (m, 2H), 1.13 – 1.11 (m, 12H), 0.95 (t, J = 7.50 Hz, 3H); ^{13}C NMR (125 MHz, $CDCl_3$) δ: 163.14, 162.99, 162.93, 144.73, 144.70, 143.17, 138.21, 136.30, 136.03, 132.42, 131.43, 131.16, 131.13, 130.47, 130.10, 129.94, 129.69, 129.53, 128.99, 128.70 128.49, 128.13, 127.91, 127.50, 127.26, 126.63, 126.27, 125.99, 125.99, 123.10, 123.03, 122.14, 121.86, 120.49, 120.36, 119.75, 119.62, 39.37, 29.26, 28.15, 23.02, 23.00, 19.41,

12.86; IR (KBr): 2960, 2868, 1701, 1660, 1587, 1577, 1355, 1238, 1151, 1058 cm^{-1}; Anal. Calcd. for $C_{50}H_{40}N_2O_4$: C, 81.94; H, 5.50; N, 3.82%. Found: C, 81.55; H, 5.27; N, 3.56%.

Preparation of 9-(4-(N-octyl)-naphthalene-1,8-dicarboximide)yl)-N-(2,6-diisopropylphenyl)-perylene-3,4-dicarboximide (4C): A solution of N-(2,6-diisopropylphenyl)-9-(tributylstannyl))perylene-3,4-dicarboximide **(2)** (0.686 g, 0.89 mmol), 4-Bromo-N-octyl-naphthalene-1,8-dicarboximide **(3C)** (0.43 g, 1.12 mmol) and $Pd(PPh_3)_4$ (10.28 mg, 0.0089 mmol) in 50 mL DMF was heated at 90 °C for 2 days. The solvent was removed under reduced pressure and the residue was purified by column chromatography (silica gel, EtOAc:petroleum ether 1 : 1) to afford compound **4C** (0.35 g, 50%) as a yellow-orange solid. m. p. 293 °C; ^{1}H NMR (500 MHz, $CDCl_3$) δ: 8.69 (d, J = 7.50 Hz, 1H), 8.67 – 8.63 (m, 2H), 8.59 – 8.56 (m, 2H), 8.51 (d, J = 8.00 Hz, 1H), 8.46 (d, J = 8.00 Hz, 2H), 7.82 – 7.77 (m, 2H), 7.61 (d, J = 8.00 Hz, 1H), 7.57 (t, J = 8.00 Hz, 1H), 7.46 – 7.40 (m, 2H), 7.36 (d, J = 8.50 Hz, 1H), 7.28 (d, J = 8.00 Hz, 2H), 4.17 (t, J = 7.50 Hz, 2H), 2.73 – 2.68 (m, 2H), 1.75 – 1.69 (m, 2H), 1.41 – 1.39 (m, 2H), 1.34 – 1.31 (m, 2H), 1.27 – 1.24 (m, 6H), 1.13 – 1.11 (m, 12H), 0.82 (t, J = 7.00 Hz, 3H) ; ^{13}C NMR (125 MHz, $CDCl_3$) δ: 164.16, 164.01, 163.97, 145.78, 145.72, 144.19, 139.25, 137.34, 137.07, 133.44, 132.46, 132.20, 132.17, 131.50, 131.12, 130.95, 130.73, 130.55, 130.00, 129.72 129.53, 129.17, 128.94, 128.52, 128.28, 127.66, 127.30, 127.01, 124.14 124.07, 123.18, 123.15, 122.89, 121.49, 120.77, 120.65, 40.67, 31.86, 29.40, 29.27, 29.18, 28.21, 27.21, 24.05, 24.03, 22.67, 14.12; IR (KBr): 2958, 2860, 1701, 1660, 1585, 1458, 1355, 1242, 1155, 756 cm^{-1}; Anal. Calcd. for $C_{54}H_{48}N_2O_4$: C, 82.21; H, 6.13; N, 3.55%. Found: C, 81.95; H, 5.87; N, 3.16%.

Preparation of 9-(4-(N-hexadecyl)-naphthalene-1,8-dicarboximide)yl)-N-(2,6-diisopropylphenyl)-perylene-3,4-dicarboximide (4D): A solution of N-(2,6-diisopropylphenyl)-9-(tributylstannyl))perylene-3,4-dicarboximide **(2)** (0.686 g, 0.89 mmol), 4-Bromo-N-hexadecyl-naphthalene-1,8-dicarboximide **(3D)** (0.55 g, 1.12 mmol) and $Pd(PPh_3)_4$ (10.28 mg, 0.0089 mmol) in 50 mL DMF was heated at 90 °C for 2 days. The solvent was removed under reduced pressure and the residue was purified by column chromatography (silica gel, EtOAc:petroleum ether 1 : 1) to afford compound **4D** (0.40 g, 50%) as a yellow-orange solid. m. p. 244 °C; ^{1}H NMR (500 MHz, $CDCl_3$,) δ: 8.69 (d, J = 7.50 Hz, 1H), 8.65 – 8.62 (m, 2H), 8.58 - 8.54 (m, 2H), 8.49 (d, J = 8.00 Hz, 1H), 8.44 (d, J = 8.00 Hz, 2H), 7.81 – 7.76 (m, 2H), 7.61 (d, J = 7.50 Hz, 1H), 7.56 (t, J = 7.50 Hz, 1H), 7.44 – 7.39 (m, 2H), 7.35 (d, J = 8.50 Hz, 1H), 7.27 (d, J = 8.00 Hz, 2H), 4.17 (t, J = 7.50 , 2H), 2.74 – 2.68 (m, 2H), 1.73 – 1.53 (m, 2H), 1.39 – 1.37 (m, 2H), 1.33 – 1.30 (m, 2H), 1.22 – 1.18 (m, 22H), 1.13 – 1.11 (m, 12H), 0.80 (t, J = 7 Hz; 3H); ^{13}C NMR (125 MHz, $CDCl_3$) δ: 163.11, 162.95, 162.91, 144.73, 144.70, 144.15, 138.21, 136.28, 136.01, 132.42, 131.40, 131.14, 131.11, 130.45, 130.10, 129.94, 129.68, 129.52, 128.98, 128.68 128.49, 128.13, 127.90, 127.50, 127.26, 126.62, 126.26, 125.98 123.09, 123.03, 122.14, 121.88, 120.49, 120.37, 119.74, 119.61,

39.63, 30.91, 28.69, 28.67, 28.67, 28.65, 28.62, 28.58, 28.41, 28.35, 28.16, 27.19, 26.18, 23.02, 23.00, 21.67, 13.10; IR (KBr): 2924, 2852, 1701, 1662, 1587, 1460, 1355, 1240, 756 cm^{-1}; Anal. Calcd. for $C_{62}H_{64}N_2O_4$: C, 82.63; H, 7.16; N, 3.11%. Found: C, 82.25; H, 6.87; N, 2.86%.

Table S1. Shows crystallographic data and refinement parameters for crystalline **NP** derivatives.

	NP-Me	**NP-Bu**	**NP-Oc**	**NP-Hd**
Formula	$C_{47}H_{34}N_2O_4$	$C_{50}H_{40}N_2O_4$	$C_{54}H_{48}N_2O_{42}$	$C_{62}H_{64}N_2O_4$
Formula wt.	690.75	732.84	788.94	901.15
Colour, shape	Red, block	Red, block	Red, block	Red, block
Dimensions, mm	0.20x0.15x0.10	0.20x0.15x0.10	0.25x0.20x0.15	0.20x0.15 x0.10
Crystal system	Triclinic	Triclinic	Triclinic	Triclinic
Space group, Z	P-1, 2	P-1, 2	P-1, 2	P-1,2
a, Å	9.353	9.147	9.168	9.151
b, Å	14.518	14.683	12.843	13.891
c, Å	15.869	15.290	18.329	19.661
α, deg	68.16	70.99	84.99	84.33
β, deg	75.46	77.37	88.54	87.82
γ, deg	83.60	84.34	79.49	78.27
V, $Å^3$	1936.0	1893.71	2113.60	2434.50
Temp, K	296	296	296	296
d_{calcd}, g/cm^{-3}	1.390	1.285	1.240	1.229
No. of reflections collected	26567	27994	30662	28490
No. of unique reflections	6684	6636	7392	7958
$2\theta_{max}$, deg	50	50	50	50
No. of parameters	515	505	601	541
*R*1, *wr*2 ($I > 2\sigma(I)$)	0.1025,0.2632	0.0378,0.1709	0.0629,0.1980	0.0692,0.3531
*R*1, *wr*2 (all data)	0.1922,0.3237	0.1191,0.2208	0.1770,0.2815	0.2223,0.4231
Goodness of fit	1.018	1.044	1.007	1.056
CCDC number	CCDC 1495388	CCDC 1495389	CCDC 1495390	CCDC 1495391

Table S2. Shows the percentage of intermolecular contacts of a molecule in crystalline **NP** derivatives from as obtained from Hirshfeld surface analysis.

Interaction	**NP-Me**	**NP-Bu**	**NP-Oc**	**NP-Hd**
C···C %	6.1	5.7	4.5	4.0
H···H %	45.1	54.1	57.9	65.1
C···H %	22.1	25.4	24.8	20.2
O···H %	13.9	13.6	11.9	9.8
N···H %	0.4	0.4	0.6	0.2
C···O %	1.0	0.4	0.3	0.3

C···N %	0.7	0.4	0.0	0.4

total percentage of intermolecular contacts ca. 89.3% (**NP-Me**), 100% (**NP-Bu)**, 100% (**NP-Oc)**, 100% (**NP-Hd).**

Table S3. Shows calculated values of charge transfer coupling corresponding to hole/electron for **NP** derivatives using B3LYP-D3/6-311G+(d,p) in Schrödinger Materials Science Suite using Jaguar DFT engine (different dimers identified for the calculation are shown in Figure S4).

Charge transfer electronic coupling (meV)	**Dimer 1**		**Dimer 2**		**Dimer 3**	
	Electron	Hole	Electron	Hole	Electron	Hole
NP-Me	71	29	34	15	--	--
NP-Bu	59	22	6	1	--	--
NP-Oc	54	132	22	3	0.1	0.01
NP-Hd	6	42	11	6	0.1	0.04

Table S4. Shows the photophysical properties of **NP** derivatives.

	$^{a}\lambda_{abs}$ (nm)	$^{a}\lambda_{f}$ (nm)	$^{a}\Phi_{f}$	$^{a}\tau_{f}$ (ns)	$^{a}k_{r}$ (x10^{8} s^{-1})	$^{a}k_{nr}$ (x10^{8} s^{-1})	$^{b}\lambda_{abs}$ (nm)	$^{b}\lambda_{f}$ (nm)	$^{b}\Phi_{f}$	$^{b}\tau_{f}$ (ns) [%]	$^{b}k_{r}$ (x10^{8} s^{-1})	$^{b}k_{nr}$ (x10^{8} s^{-1})
NP-Me	234	541	0.78 ± 0.01	3.59	2.17	0.61	350-650	645	0.21 ± 0.02	1.45 [68] 3.08 [32]	0.93	3.49
NP-Bu	234	540	0.82 ± 0.01	3.54	2.32	0.51	350-620	644	0.47 ± 0.02	1.22 [70] 4.46 [30]	1.47	1.66
NP-Oc	234	539	0.80 ± 0.01	3.54	2.26	0.56	350-600	621	0.18 ± 0.02	1.95 [45] 5.25 [55]	0.40	1.83
NP-Hd	233	539	0.83 ± 0.01	3.49	2.38	0.49	350-590	591	0.24 ± 0.02	1.12 [61] 3.17 [39]	0.74	3.36

[a]chloroform solution; [b]crystalline state; abs – absorption; f – fluorescence; Excitation wavelength for fluorescence emission, 475 nm; Fluorescence lifetime (Excitation wavelength, 439 nm and emission collected at 550 nm for NP-Me, NP-Bu, NP-Oc and NP-Hd in $CHCl_3$ solution and 640 nm for NP-Me and NP-Bu, 620 nm for NP-Oc and 590 nm for NP-Hd in the crystalline state)

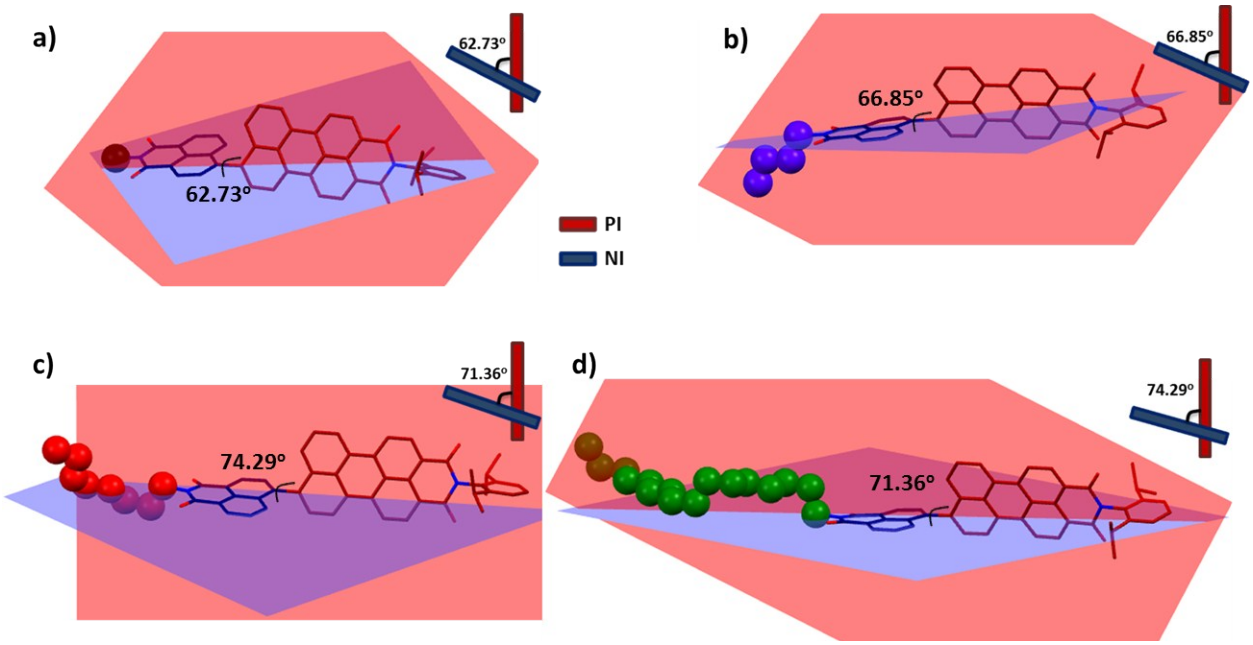

Fig. S1. Shows the angle between planes of NI and PI units of **NP** derivatives in the crystalline state of a) **NP-Me**, b) **NP-Bu**, c) **NP-Oc** and d) **NP-Hd**. Hydrogens are omitted for clarity. Schematic represents the orientation of the PI and NI planes when viewed along the single covalent bond connecting the two units.

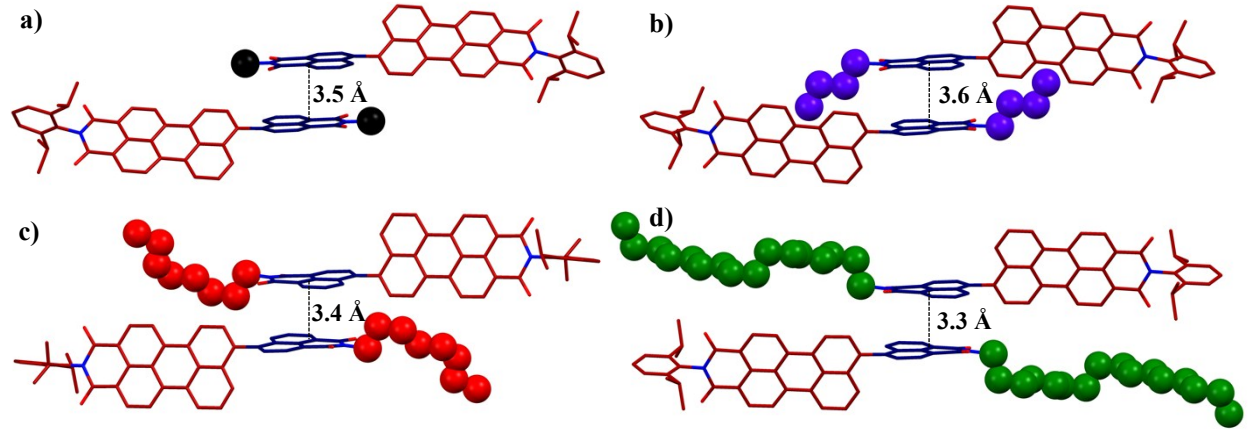

Fig. S2. Shows the distance between NI units of adjacent **NP** derivatives in the crystalline state of a) **NP-Me**, b) **NP-Bu**, c) **NP-Oc** and d) **NP-Hd**. Hydrogens are omitted for clarity.

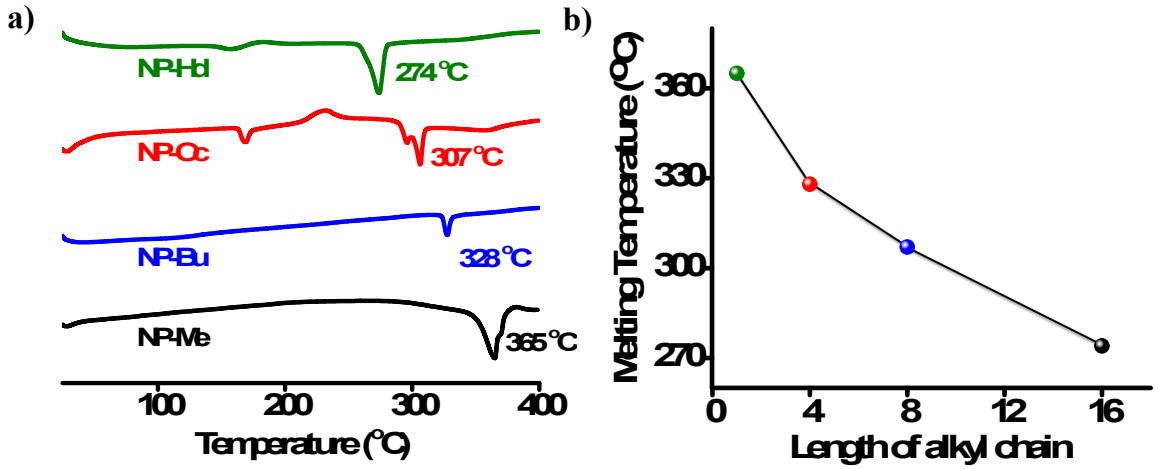

Fig. S3. a) DSC analysis of the derivatives **NP-Me**, **NP-Bu**, **NP-Oc** and **NP-Hd**; b) near-linear decrease in melting temperature of **NP** derivatives plotted against the number of carbon atoms in the alkyl side-chain.

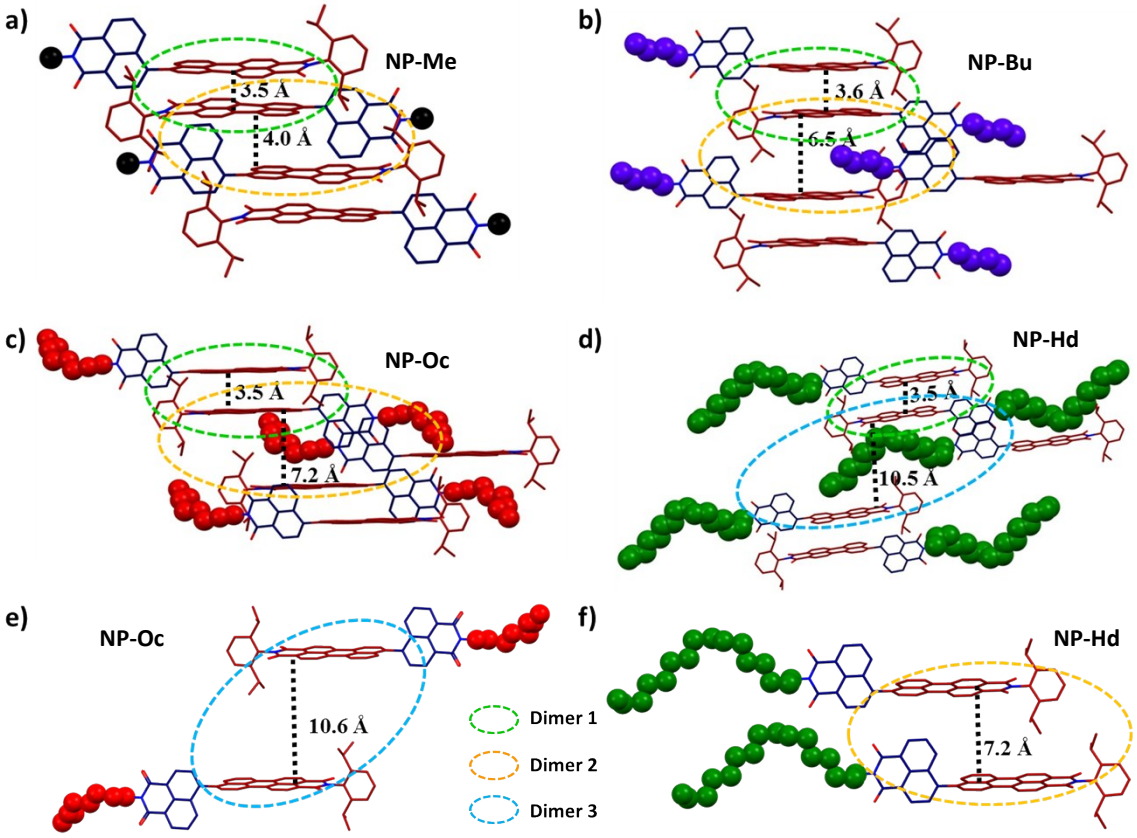

Fig. S4. Shows the dimers identified for calculation of charge transfer coupling corresponding to hole/electron for **NP** derivatives using B3LYP-D3/6-311G+(d,p) in Schrödinger Materials Science Suite using Jaguar DFT engine.

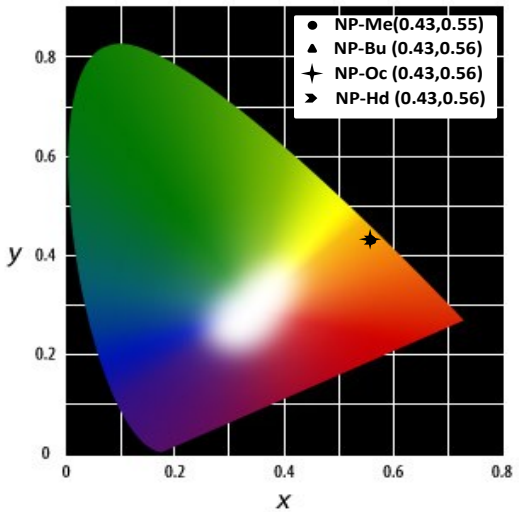

Fig. S5. Shows CIE colour diagram of fluorescence emission for **NP** derivatives in solution state ($CHCl_3$).

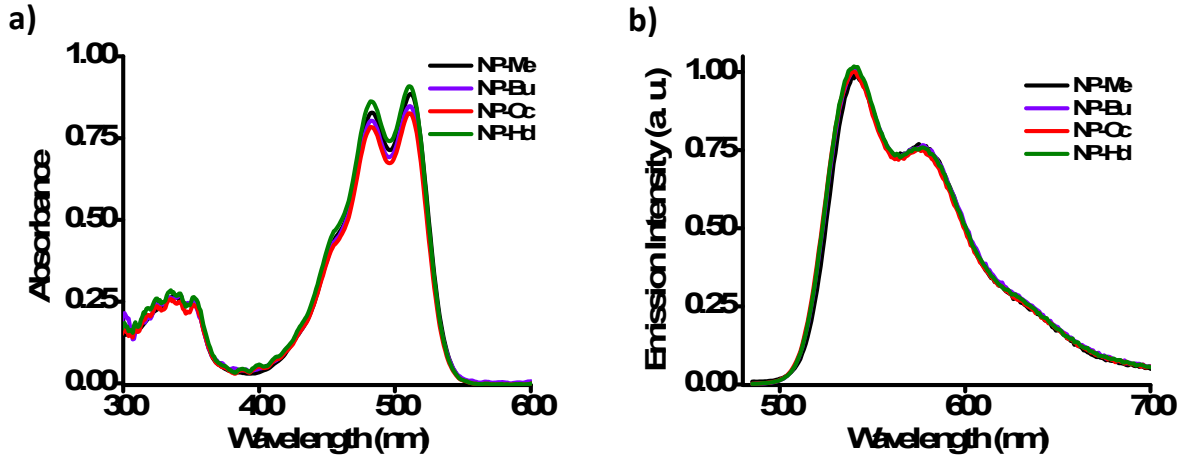

Fig. S6. Shows a) absorption and b) emission spectra of **NP** derivatives in $CHCl_3$.

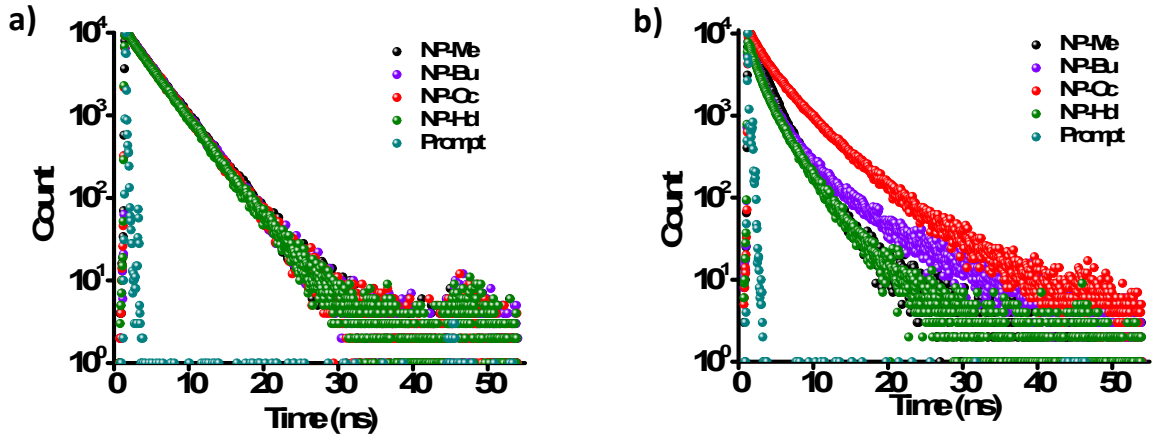

Fig. S7. Shows fluorescence decay profile of **NP** derivatives in a) $CHCl_3$ solution and b) crystalline state on exciting at 439 nm and collected at the respected emission maxima.

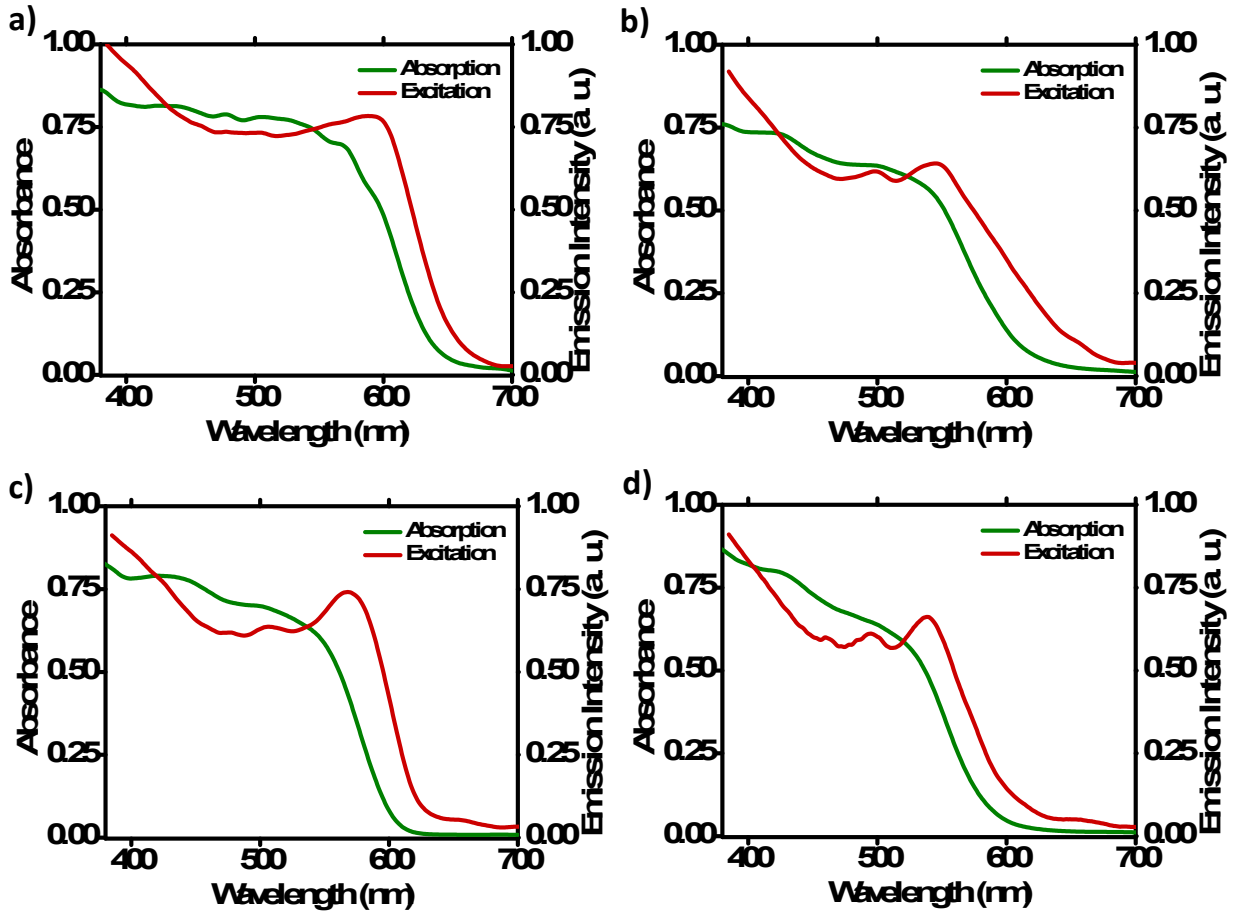

Fig. S8. Shows the fluorescence excitation spectra of a) **NP-Me**, b) **NP-Bu**, c) **NP-Oc** and d) **NP-Hd** in crystalline state as compared to their respective absorption spectra.

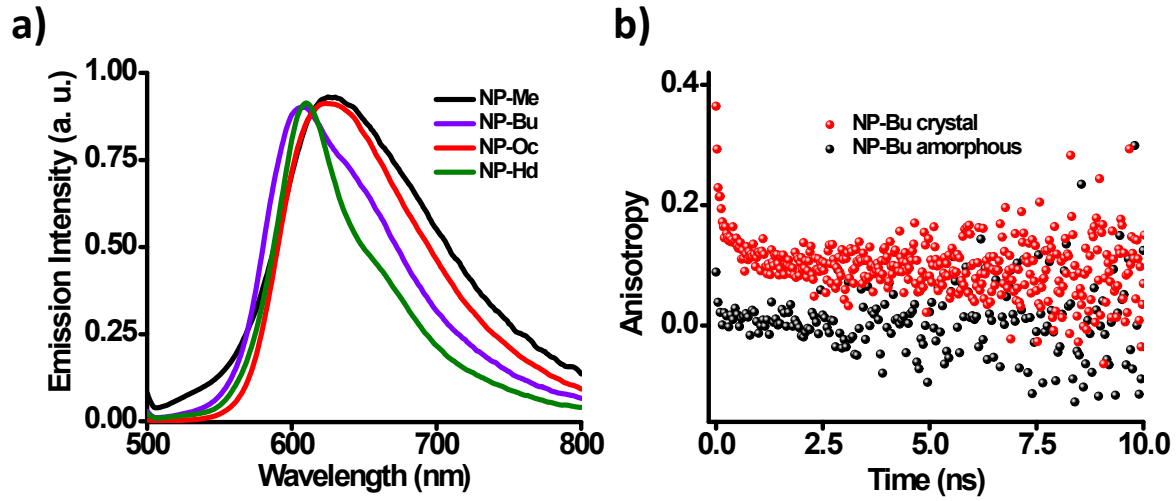

Fig. S9. Shows fluorescence emission spectra of a) **NP** derivatives in amorphous state; b) fluorescence anisotropy decay of **NP-Bu** as a representative example of **NP** derivatives in amorphous state compared to that in the crystalline state.

References

1. D. L. Sackett and J. Wolff, *Anal. Biochem.*, 1987, **167**, 228-234.
2. M. Cölle, J. Gmeiner, W. Milius, H. Hillebrecht and W. Brütting, *Adv. Funct. Mater.*, 2003, **13**, 108-112.
3. J. R. Lakowicz, *Principles of Fluorescence Spectroscopy*, Springer US, 2007.
4. A. D. Bochevarov, E. Harder, T. F. Hughes, J. R. Greenwood, D. A. Braden, D. M. Philipp, D. Rinaldo, M. D. Halls, J. Zhang and R. A. Friesner, *Int. J. Quantum Chem.*, 2013, **113**, 2110-2142.
5. W.-Q. Deng and W. A. Goddard, *J. Phys. Chem. B*, 2004, **108**, 8614-8621.
6. R. T. Cheriya, J. Joy, A. P. Alex, A. Shaji and M. Hariharan, *J. Phys. Chem. C*, 2012, **116**, 12489-12498.